http://dx.doi.org/10.5516/NET.09.2011.057

〈Technical Note〉

VIBRATION AND STRESS ANALYSIS OF A UGS ASSEMBLY FOR THE APR1400 RVI CVAP

DO-YOUNG KO* and KYU-HYUNG KIM
Central Research Institute, Korea Hydro and Nuclear Power Co., Ltd.
70, 1312 beon-gil, Yuseong-daero, Yuseong-gu, Daejeon, 305-343, Republic of KOREA
*Corresponding author. E-mail : kodoyoung@khnp.co.kr

Received October 19, 2011
Accepted for Publication January 26, 2012

The most important component of a nuclear power plant is its nuclear reactor. Studies on the integrity of reactors have become an important part regarding the safety of a nuclear power plant. The US Nuclear Regulatory Commission Regulatory Guide (NRC RG) 1.20 presents a Comprehensive Vibration Assessment Program (CVAP) to be used to verify the structural integrity of the Reactor Vessel Internals (RVI) for flow-induced vibration prior to commercial operation. However, there are few published studies related to the RVI CVAP. We classified the Advanced Power Reactor 1400 (APR1400) RVI CVAP as a non-prototype category-2 reactor as part of an independent validation of its design. The aim of this paper is to present the results of structural response analyses of the Upper Guide Structure (UGS) assembly of the APR1400 reactor. These results show that the UGS and the Inner Barrel Assembly (IBA) meet the specified integrity levels of the design acceptance criteria. The vibration and stress analysis results in this paper will be used as basic information to select measurement locations of the vibration and stress for the APR1400 RVI CVAP.

KEYWORDS : APR1400, RVI, CVAP, Vibration and Stress, UGS Assembly

1. INTRODUCTION

The integrity of reactors has always been an important issue regarding the safety of a nuclear power plant. Prior to commercial operation, one of the foremost means of verifying the integrity of a reactor is through the Reactor Vessel Internals Comprehensive Vibration Assessment Program (RVI CVAP) of the US Nuclear Regulatory Commission Regulatory Guide (NRC RG) 1.20 [1]: Comprehensive Vibration Assessment Program for Reactor Internals during Preoperational and Initial Startup Testing. The CVAP is composed of a vibration and stress analysis, vibration and stress measurement, and inspection programs that operate in conjunction with verification of the structural integrity, to establish a feasible margin of safety [1]. The classification of the RVI relative to the CVAP is determined by the design, operating parameters, and operating experience with a number of potential prototypes. A summary and more information about the CVAP category are described in the US NRC RG 1.20 [1].

The Advanced Power Reactor 1400 (APR1400) RVI CVAP was classified as a non-prototype category-2 reactor as part of an independent validation of its design [2-6]. The assessment of a non-prototype category-2 reactor includes an analysis, limited measurements, and a full inspection.

The RVI components are largely classified into three categories: the Core Support Barrel (CSB), the Lower Support Structure (LSS) / Core Shroud (CS) and the Upper Guide Structure (UGS) [7]. However, the UGS assembly of the APR1400 RVI was designed for a structure having more improved integrity as the assembly of the UGS and the Inner Barrel Assembly (IBA). Limited measurements mean that one, two, or three components can be measured as part of the vibration and stress measurement program of the RVI CVAP.

In this paper, the vibration and stress analysis results of the UGS and the IBA for the APR1400 RVI CVAP are presented for a theoretical integrity verification given the presence of flow-induced vibration and the potential adverse flow effects on the reactor.

This paper will show that the UGS and the IBA secure integrity against flow-induced vibration. However, these structures need to be chosen as components for the vibration and stress measurement program of the non-prototype category 2 for the APR1400 RVI CVAP. In a future study, the vibration and stress analysis results in this paper will be applied to the determination of the measurement locations of the instruments.

2. VIBRATION AND STRESS ANALYSIS

2.1 Modeling

The analysis method applied in this study involves a calculation of the structural response using a three-dimensional finite element method. The analysis models by the three-dimensional finite element method are made using the geometry models of the UGS and the IBA [8, 12].

The three-dimensional geometric models were initially generated using a 3D CAD program (Pro/Engineer) with the actual dimensions. The geometric models were then simplified within a range that did not affect the analysis results. Third, meshes of the geometric models were generated using a structural analysis program (ANSYS). Fig. 1 shows the UGS and the IBA analysis models.

The UGS model mainly uses a hexahedral mesh due to the tube banks of the lower UGS. The Fuel Alignment Plate (FAP) model of the UGS uses a tetrahedral mesh considering its complicated geometry. The IBA mainly uses a hexahedral mesh due to its regular geometry. A SOLID186 element was used to calculate the stress/strain or displacement, and a SURF154 element was applied to consider the additional masses on the surfaces of the structures.

In the generated analysis model, the UGS has approximately 1,300,000 nodes and the LSS has about 900,000.

2.2 Boundary Conditions

Constraints are important factors when determining the accurate structural response because they limit the strain on the structures and affect their stiffness. Therefore, we established more realistic constraint conditions referring to the RVI part and assembly drawings.

The upper flange of the UGS assembly is fixed with a hold-down ring and the upper flange of the CSB assembly, when the reactor vessel is assembled with a reactor upper head; thus, the Degrees of Freedom (DOFs) in the vertical and circumferential direction at the upper UGS assembly are fixed. The circumferential DOF at the lower UGS assembly is fixed as well due to the assembly between the four grooves of the FAP and the guide lugs of the upper CS.

The Control Element Assembly (CEA) shroud assembly in an Optimized Power Reactor 1000 (OPR1000) is fixed to the UGS bottom plate owing to a method that utilizes tie-rods and CEA shroud rings. However, the CEA shroud assembly in the APR1400 is fixed to a cylinder, due to the introduction of the IBA. Therefore, all DOFs at the upper IBA are fixed and the outside CEA shroud is welded to the inside of the IBA cylinder. This IBA allows a change of the transmittal path of seismic loads and a change of the structural responses of the IBA by hydraulic loads. Therefore, the vibration characteristics of the IBA under the normal operating conditions are important concerns in this study.

As noted earlier, given the present boundary conditions, we carried out a vibration and stress analysis of each component, as an individual analysis simplified the analysis overall and reduced the analysis time.

The behavior of the structures in a reactor differs from that in air owing to the reactor coolant; the inertia of the structures increases due to the coupling effects of the fluid and solid components. To consider this different condition, the mass added to each structure was calculated using the ASME Boiler & Pressure Vessel (B & PV) Code.

Based on the US NRC RG 1.20, we consequently applied a 1% damping factor for a conservative analysis. If structural damping factors greater than 1% are to be used, the suitability should be strongly substantiated with vibration and stress measurements [1].

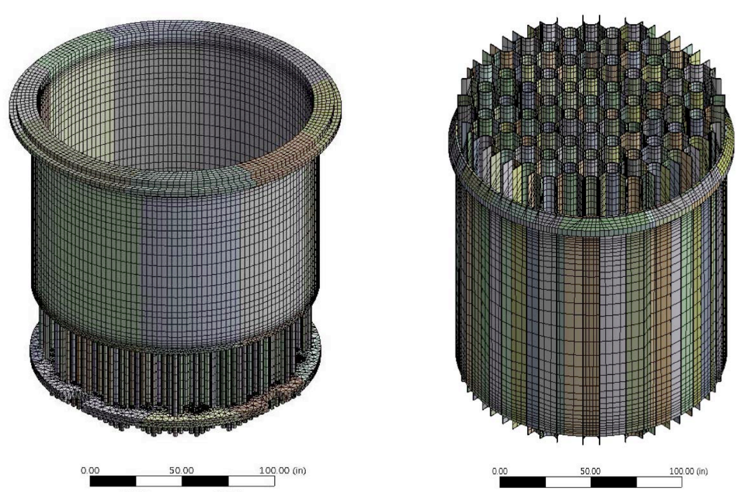

(a) Upper guide structure (b) Inner barrel assembly

Fig. 1. Analysis Models of the UGS and IBA

In this study, the material applied for the vibration and stress analysis is austenitic stainless steel. The basic properties were selected after referring to the ASME B & PV Code. Table 1 shows material properties of the UGS and the IBA.

2.3 Modal Analysis

A modal analysis served to elucidate the dynamic characteristics of the structures for the response analysis. In this study, a superposition method using the block Lanczos method was used to determine the natural frequencies and mode shapes of the UGS and the IBA.

As shown in Table 2, the UGS generated the first mode at 13.39 Hz in coolant, showing a typical shell type of cylinder structures. From the third mode, the UGS had compound plate and shell types. These are shown in Figs. 2 (a) and (b).

Also shown in Table 2, the IBA took the first mode at 33.22 Hz in coolant and had a shell type. But, from the second mode, the IBA showed that the cylinder and CEA guide tubes plate had a simultaneously complex shell and plate types. These are shown in Fig. 2 (c) and (d).

The data in Table 2 were used to predict and judge the resonance and behavior of the structures when under loads.

Table 1. Material Properties of the UGS and IBA

Modulus of elasticity	29,000 ksi
Density	0.289 lb/in^3
Poison's ratio	0.29
Damping ratio	0.01

Table 2. Natural Frequencies and Mode Types of UGS and IBA

	UGS		IBA	
	Frequency	Mode type	Frequency	Mode type
1st	13.39 Hz	shell	33.22 Hz	shell (cylinder)
2nd	14.35 Hz	plate	36.26 Hz	complex
3rd	32.24 Hz	complex	63.44 Hz	complex
4th	72.18 Hz	complex	79.97 Hz	complex
5th	107.52 Hz	complex	99.88 Hz	complex

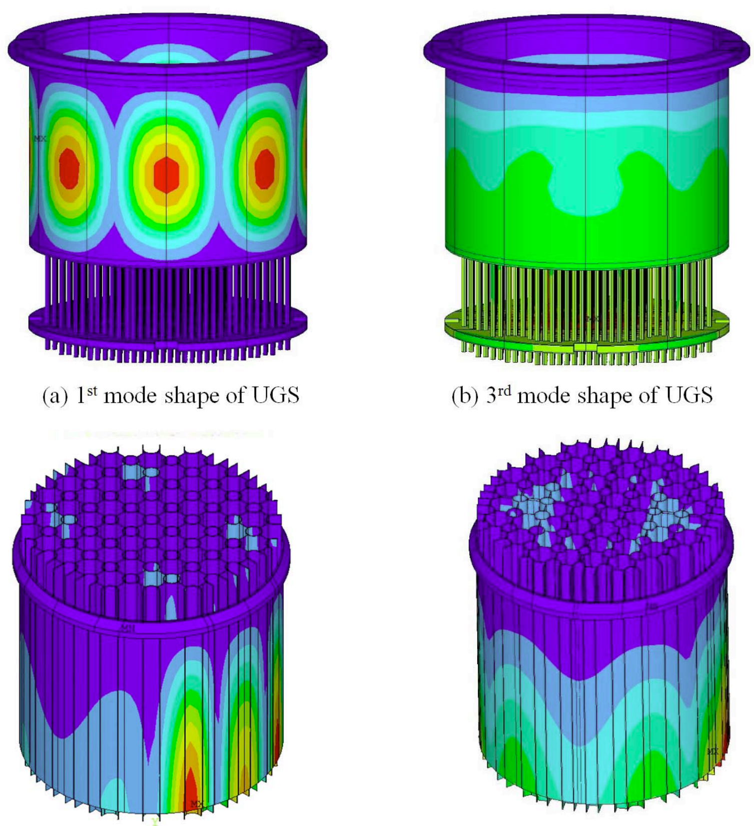

(a) 1st mode shape of UGS (b) 3rd mode shape of UGS

(c) 1st mode shape of IBA (d) 2nd mode shape of IBA

Fig. 2. Mode Shapes of the UGS and IBA

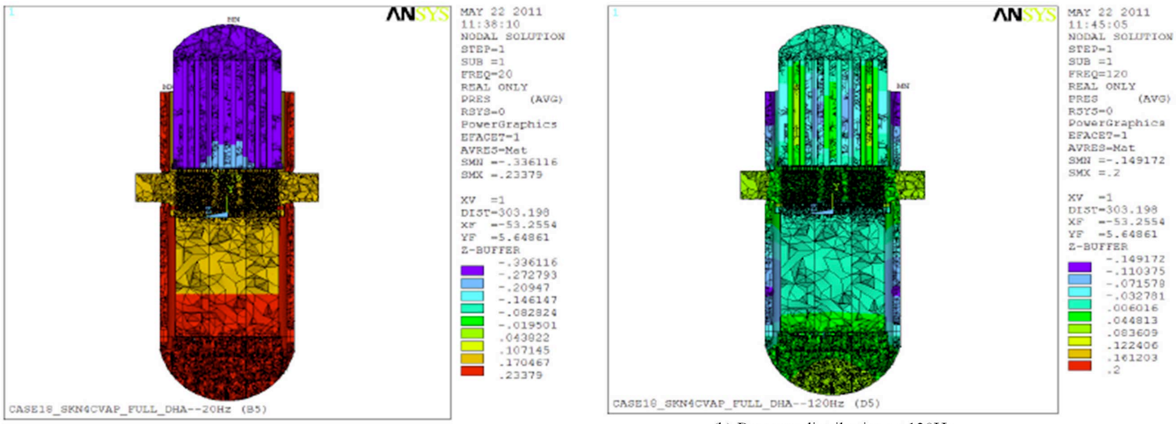

(a) Pressure distribution at 20Hz (b) Pressure distribution at 120Hz

Fig. 3. Pressure Distribution on the RVI Assembly [psi]

2.4 Structural Response Analysis

To calculate the structural response to an external force, the specific characteristics of the external force should initially be determined. The hydraulic forcing function of the RVI CVAP consist of two hydraulic loads according to the source of excitation: the first is a periodic hydraulic load caused by the pressure pulsation of the Reactor Coolant Pump (RCP), and the second is a random hydraulic load caused by a turbulent flow [9, 10, 11]. These hydraulic loads depend on the analysis temperatures/pressures and the RCP operating conditions.

In this paper, an RVI CVAP analysis condition involving the highest temperature/pressure with four RCPs was selected. In addition, this case has the largest flow rate amounts surrounding the RVI. The vibration and stress analysis conditions in this study are shown in Table 3.

Table 3. Analysis Conditions in the Study Case

Number of RCPs	4 pumps
Temperature	555 ºF
Pressure	2,220 psi
Mass flow rate	11,563 lb/s per pump

2.4.1 Periodic Response Analysis

The hydraulic load caused by the pressure pulsation of the RCP is a periodic load of which the frequency is determined by the rotor frequency (20 Hz) and the blade-passing frequency (BPF: 120 Hz). Determination of the structural response for the periodic load was carried out via a harmonic analysis using ANSYS. The periodic loads include a total of six frequencies: 20 Hz, 40 Hz, 120 Hz, 240 Hz, 360 Hz and 480 Hz. These frequencies are mainly multiples of 20 Hz and 120 Hz [7, 8].

Fig. 3 shows the pressure distribution at 20 Hz and 120 Hz in the reactor vessel. The pressure loads depend upon the cycle and the size of each pressure wave. When the reactor coolant moves up to the IBA following the flow path, the pressure is gradually reduced because the periodic loads are transmitted by acoustic waves with regular frequencies. High absolute values were noted at the peak and valley points of each pressure wave. In Fig. 3 (a), the pressure wave shows negative values around the UGS tube bank, because the pressure wave moves up to the IBA in a manner that generates valley points. Fig. 3 (b) shows the pressure distribution at 120 Hz. These pressure changes appear more often than that in Fig. 3 (a) because the wavelength is shorter.

All pressures taken at the six aforementioned frequencies were applied to the surface nodes of the components with SOLID186 elements. The structural responses of the UGS and the IBA were then determined from a calculation of each load at the six frequencies after the analysis conditions; i.e., the constraints, the added masses and other parameters were kept equal to those in the modal analysis.

Figs. 4 and 5 depict the results of the periodic responses of the UGS and the IBA at each frequency. As shown in Fig. 4, in the UGS, the locations with the highest stresses were the lower UGS tube bank and the FAP. The area around the four grooves of the FAP had relatively high stress levels owing to the assembly between the four grooves of the FAP and the guide lugs of the upper CS.

Regarding the periodic responses of the IBA in Fig. 5, the locations with high stress levels were between the inside of the IBA cylinder and the outside of the CEA guide tubes. These locations appear to be relatively weak structural points, as high stress was generated between these components.

2.4.2 Random Response Analysis

The amplitude and frequencies of the hydraulic loads caused by a turbulent flow showed a typical Power Spectral

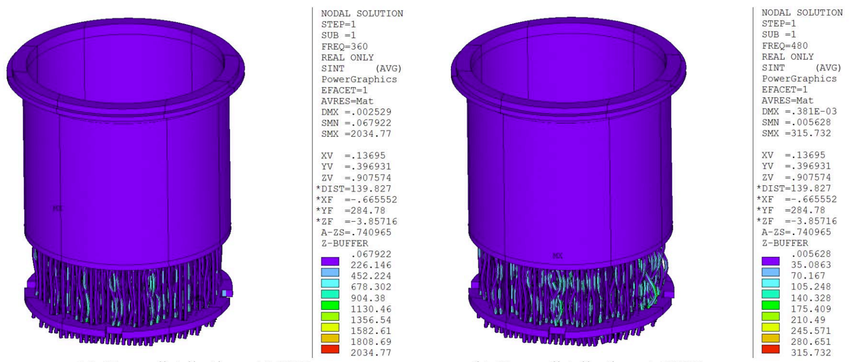

(a) Stress distribution at 360Hz (b) Stress distribution at 480Hz

Fig. 4. Periodic Response of the UGS [psi]

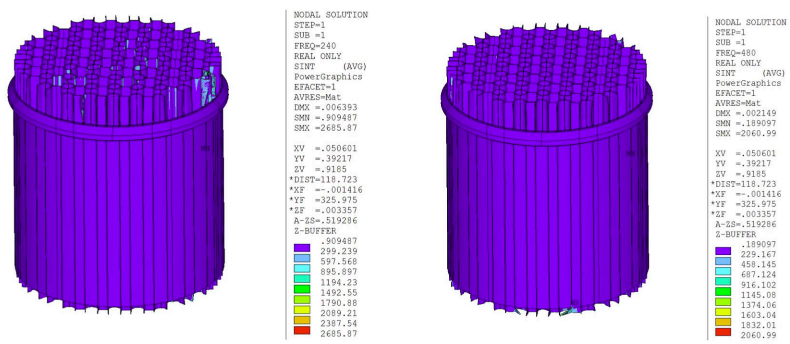

(a) Stress distribution at 240Hz (b) Stress distribution at 480Hz

Fig. 5. Periodic Response of the IBA [psi]

Density (PSD) as a consequence of random characteristics. The structural responses of the random hydraulic loads were determined from a calculation using the spectrum analysis of ANSYS [8]. The frequency ranges of the random loads were set to range from 0 to 500 Hz considering the maximum frequency (480 Hz) of the periodic loads.

The periodic responses were calculated using the loads classified by the nodes; however, the random responses were calculated by the loads of the divided areas. For a conservative analysis, this was done using the maximum value from among many PSD loads sampled from areas that showed a similar flow distribution.

The APR1400 design materials specify that the inflow rate to the UGS from the main flow should be less than 3%. The gap between the inside of the UGS cylinder and the outside of the IBA cylinder is very small. Consequently, the flow at the gap is assumed to have a very small flow rate. Based on this assumption, the loads at the UGS assembly were applied at the FAP, the CEA guide tube bank, and the UGS bottom plate.

Figs. 6 and 7 show the areas divided by the flow distribution of the UGS assembly. The UGS assembly was split into three parts: the CEA guide tube bank, the UGS bottom plate, and the FAP.

The CEA guide tube bank was again divided into the upper region and the lower region on the basis of the FAP. The upper region of the CEA guide tube bank was divided into 19 areas, and the lower region of this tube bank was divided into 9 areas. Therefore, the CEA guide tube bank had a total of 28 areas, as shown in Figs. 6 (a) and (b). The PSDs of the representative loads, depending on the areas, were also obtained, as shown in Figs. 8 (a) and (b). The UGS bottom plate and FAP were respectively divided horizontally into 9 areas, as shown in Figs. 7 (a) and (b). The PSDs of the representative loads by areas were then obtained, as shown in Figs. 9 (a) and (b). The total number of areas divided according to the flow distribution of the UGS assembly is, therefore, 46.

The PSD data were generated using 512 velocity values with 0.001-second intervals. The UGS and the IBA of the analysis time had intervals of 5 ~ 6.5 seconds.

The random responses of each area yielded to the PSD, as the input values were random data. These random responses are presented with variances after integrating the PSD data, because the random responses follow a Gaussian distribution. Therefore, the random responses have a probability of 99.73% with 3σ of stress and 3σ of strain, where σ denotes the standard deviation. This is estimated as a practically conservative result given the responses with random input values. Fig. 10 presents the UGS and IBA stress distribution in a 3σ scale.

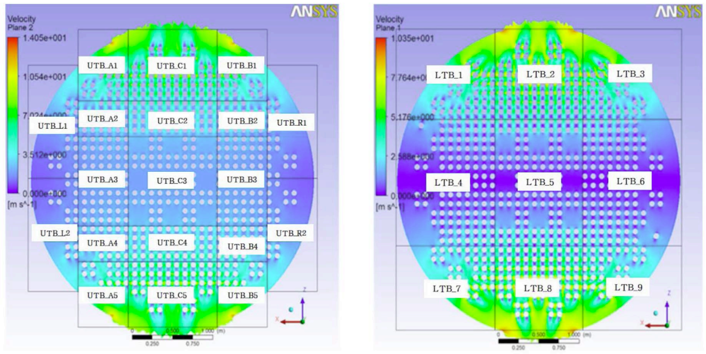

(a) CEA guide upper tube bank (b) CEA guide lower tube bank

Fig. 6. Area Divided by the Flow Distribution of the CEA Guide Tube Bank

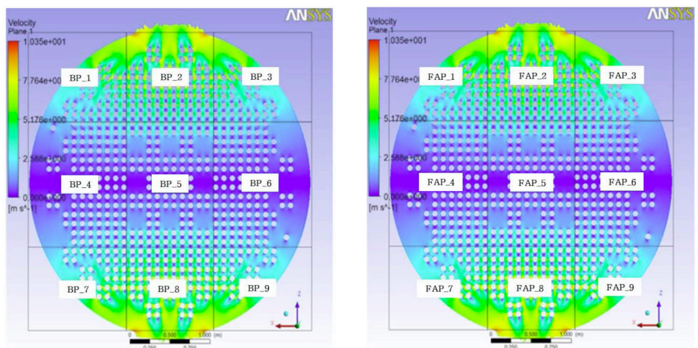

(a) UGS bottom plate (b) FAP

Fig. 7. Area Divided by the Flow Distribution of the UGS Bottom Plate and the FAP

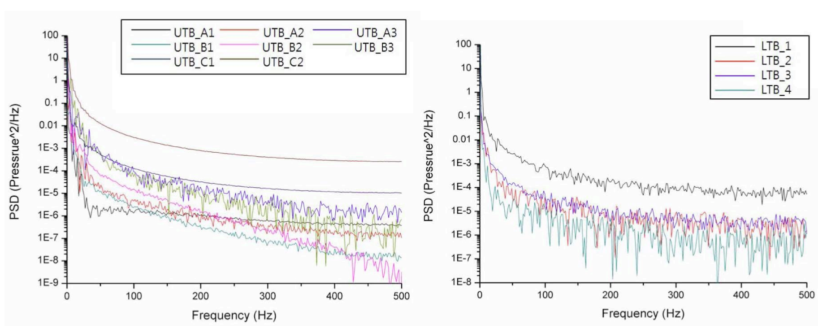

(a) PSDs of the CEA guide upper tube bank (b) PSDs of the CEA guide lower tube bank

Fig. 8. Random Loads of the CEA Guide Tube Bank

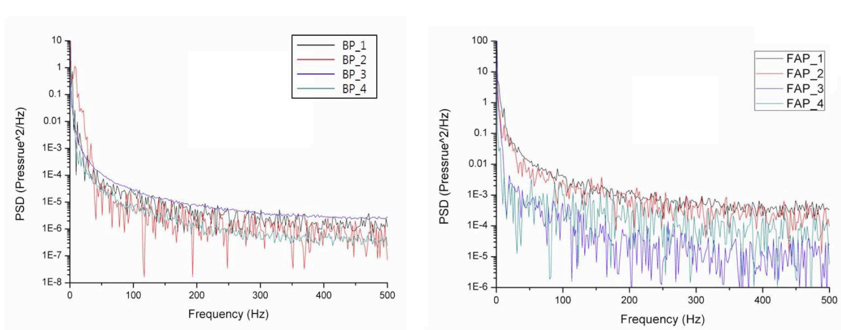

(a) PSDs of the UGS bottom plate (b) PSDs of the FAP

Fig. 9. Random Loads of the UGS Bottom Plate and the FAP

Table 4. Stress Results of the UGS and IBA [psi]

Component	Periodic response						Random response (3σ)	Total response
	20 Hz	40 Hz	120 Hz	240 Hz	360 Hz	480 Hz		
UGS	102.35	20.35	26.79	62.40	2034.77	315.73	46.12	2063.40
IBA	205.36	16.57	21.92	2685.87	513.56	2060.99	3205.36	4694.95

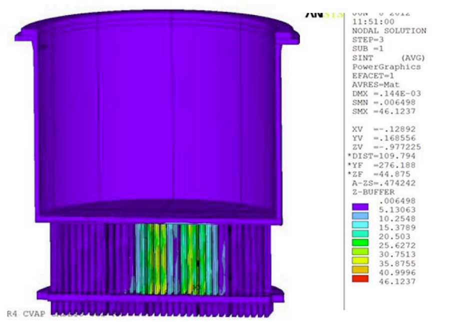

(a) Stress (3σ) distribution of the UGS

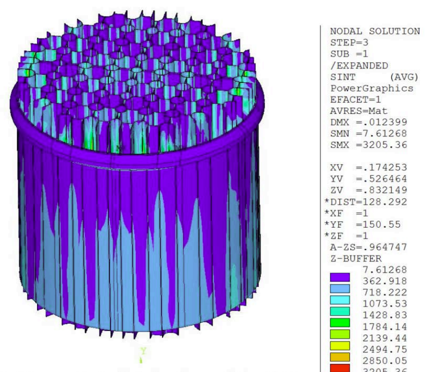

(b) Stress (3σ) distribution of the IBA

Fig. 10. Random Responses of the RVI [psi]

2.5 Combination of Responses

The stress intensities generated at the UGS and the IBA are shown in Table 4. The values in Table 4 are the peak values under the analysis conditions. The total responses were combined by the Square Root of the Sum of Squares (SRSS) method.

In the case of the UGS, the summed structural response is mainly caused by the periodic hydraulic load at the 360 Hz. This indicates that the UGS responds more to a pump pulsation load than to a random load. On the other hand, total response of the IBA has a similar rate for a periodic load and a random load.

As shown in Table 4, the IBA had greater stress than the UGS. Therefore, the IBA had a lower margin than the UGS, given the amount of stress under the same operating conditions.

Table 5. Peak Stresses and Fatigue Margins

Component	Peak stress [psi]	Endurance limit [psi]	Fatigue margin
UGS	2063.40	13,600	6.59
IBA	4694.95	13,600	2.90

3. EVALUATION OF THE STRUCTURAL INTEGRITY

The loads applied to the structures considered in this study are dynamic loads. Therefore, fatigue damage must be factored in when evaluating the integrity of all components. That is to say, after the establishment of acceptance limits, the peak stresses generated at the structures should be judged as to whether or not they exceed the acceptance limits.

The design fatigue curve (S-N curve) in the ASME B & PV code presents the fatigue strength according to the load cycle and material. For a conservative evaluation in this study, the endurance limit at the 10^{11} cycle was set as the allowable fatigue strength. Austenitic steel was used as the material of the structures.

Table 5 shows a comparison of the endurance limit and the peak stress of the UGS and the IBA. The fatigue margin is calculated by dividing the endurance limit from the peak stress. Therefore, the fatigue margins of the UGS and the IBA were respectively confirmed at 6.59 and 2.90, given the endurance limit of 13.6 ksi. This implies that a fatigue fracture will not occur for a period of 60 years.

4. DISCUSSION

The vibration and stress analysis program of the RVI CVAP is utilized as a means of theoretical verification of the structural integrity and for the selection of the appropriate vibration and stress measurement locations. As noted in the introduction to this paper, the non-prototype category 2 involves an analysis, limited measurements, and a full inspection. Therefore, the APR1400 RVI CVAP using the non-prototype category 2 should be selected for one or more structures in the RVI for limited measurements [2, 3, 4]. The response results in the present study show that the UGS and the IBA possess the necessary levels of structural integrity. Specifically, the fatigue margin of the

UGS and the IBA are 6.59 and 2.90, respectively; however, these structures can be included as components in the measurement program of the non-prototype category 2 for the APR1400 RVI CVAP.

In earlier research related to the APR1400 RVI CVAP, Ko determined the selection criteria of the measurement locations for the APR1400 RVI CVAP [3, 4] and affirmed that the arrangement and size of the CSB and the LSS of APR1400 are nearly identical, compared to a valid prototype (the Palo Verde Nuclear Generating Station Unit 1, PVG #1). However, the UGS assembly design was altered for better integrity, made possible by a change in the loads path of the CEA shroud. Moreover, the design and operating conditions of the APR1400 are quite similar to that of the valid prototype, except for the increase in the thermal capacity (6 %) and the increase in the operating coolant flow rate (1.56%). The vibration and stress measurement results of the PVG #1 RVI CVAP demonstrate that the measured values are very low in comparison to the test acceptance criteria. Therefore, Ko asserted [3, 4] that when the vibration and stress measurement programs of the APR1400 RVI CVAP are used, the CSB and the LSS can be omitted, and the UGS assembly can instead be selected.

In a future study, it will be necessary to verify whether or not the integrity of the APR1400 design requires additional analyses related to other structures. This pertains expressly to the CSB and the LSS components.

5. CONCLUSION

In this paper, the structural integrity levels of the UGS and the IBA of the APR1400 design were assessed using the vibration and stress analysis program of the RVI CVAP. In comparison with the response stresses by hydraulic loads and the fatigue margins of the materials, the UGS and the IBA present fatigue margins at 6.59 and 2.90, respectively.

The vibration and stress analysis results of the UGS and the IBA as determined in the present study indicate that the expected values are much smaller than the design acceptance criteria. Therefore, the UGS and the IBA are judged to secure a feasible level of integrity against dynamic loads in the analysis case (555 °F, 2220 psi and four reactor coolant pumps in operation). However, when the vibration and stress measurement program for the APR1400 RVI CVAP is conducted, the UGS assembly needs to be included. These results will be used to select CVAP measurement locations for the APR1400 RVI CVAP. The next part of this study regarding the APR1400 design validation will be performed.

REFERENCES

[1] US Nuclear Regulatory Commission, "Comprehensive Vibration Assessment Program for Reactor Internals during Preoperational and Initial Startup Testing," Regulatory Guide 1.20, Rev.0 (2007).

[2] D. Y. Ko and J. G. Lee, "A Review of Measuring Sensors for Reactor Vessel Internals Comprehensive Vibration Assessment Program in Advanced Power Reactor 1400," Transactions of Korean Society for Noise and Vibration Engineering, Vol. 21, No. 1, pp. 47-55 (2011).

[3] D. Y. Ko, K. H. Kim and S. H. Kim, "Selection Criteria of Measurement Locations for Advanced Power Reactor 1400 Reactor Vessel Internals Comprehensive Vibration Assessment Program," Transactions of Korean Society for Noise and Vibration Engineering, Vol. 21, No. 8, pp. 708-713 (2011).

[4] D. Y. Ko, K. H. Kim and S. H. Kim, "Response Instrumentation Test Acceptance Criteria for APR1400 RVI CVAP," Transactions of Korean Society for Noise and Vibration Engineering, Vol. 21, No. 11, pp. 1036-1042 (2011).

[5] D. Y. Ko, K. H. Kim and S. H. Kim, "Structural Analysis and Response Measurement Locations of Inner Barrel Assembly Top Plate in APR1400," Transactions of Korean Society for Noise and Vibration Engineering, Vol. 22, No. 5, pp. 474-479 (2012).

[6] K. H. Kim, D. Y. Ko and S. H. Kim, "Vibration Stress Analysis for Reactor Vessel Internals of Advanced Power Reactor 1400 by Pulsation of Reactor Coolant Pump," Transactions of Korean Society for Noise and Vibration Engineering, Vol. 21, No. 12, pp. 1098-1103 (2011).

[7] D. Y. Ko and J. G. Lee, "Development of a remote measurement system for the gap between RV and CSB for RVI-modularization," Nucl. Eng. Des, Vol. 240, pp. 2907-2913 (2010).

[8] K. H. Kim, D. Y. Ko and Y. S. Kim, "Hydraulic and Structural Analysis Methodology of RVI CVAP in Shin-Kori 4," Transaction of the Korean Nuclear Society Spring Meeting, Jeju, Korea, May 18-23, 2009.

[9] K. H. Kim, D. Y. Ko and J. Y. Gu, "Deterministic Hydraulic Load Analysis on Reactor Internals of APR1400," Transaction of the Korean Nuclear Society Spring Meeting, Taebaek, Korea, May 26-27, 2011.

[10] J. Y. Gu, K. H. Kim and Y. J. Choi, "Structural Response of APR1400 CSB to Pressure Pulsation of RCP," Proceeding of Korean Society of Safety, Wonju, Korea, May 19-20, 2011

[11] K. H. Kim, Y. S. Kim and D. Y. Ko "Evaluation of Detached Eddy Simulation Applicability to Random Hydraulic Load Analysis for Reactor Vessel Internals," Transaction of the Korean Nuclear Society Spring Meeting, Jeju, Korea, Oct. 21-22, 2010.

[12] J. Y. Gu, K. H. Kim and Y. S. Kim, "Development and Validation of Structural Analysis Methodology for Comprehensive Vibration Assessment for Reactor Vessel Internals," Proceeding of the Korean Society of Mechanical Engineers, Jeju, Korea, Nov. 3-5, 2010.